

Real-time navigation system for Central Venous Catheters using ultrasound technology

Dejana Vuković, Dr. Jens Wildhagen, M.Eng. Korbinian Köhler

Abstract—In this paper the development and testing of a system prototype for a novel real-time navigation using 100 kHz ultrasound technology intended for the precise positioning of a CVC (Central Venous Catheter) inside the central venous system is presented. For the prototype realization a DSP (Digital Signal Processor) based hardware, including data converters, an ultrasonic transducer and a hydrophone, has been used. The processing algorithms implemented in C programming language included amplitude modulation/demodulation, matched filtering, and polyphase interpolation of chirp signals. For testing purposes, a measurement setup with a model of the upper part of the human torso based on water, agar-agar, pork ribs and pork lung was established. This paper shows the results of testing the developed prototype in terms of robustness, accuracy, and the possibility of ultrasound transmission through tissue, lungs, and ribs. The presented results indicate that even though the developed system shows a high level of accuracy (> 98 %) with a distance estimation update rate of 3.2 s and a usability for distances up to 20 cm in case of transmission through tissue and ribs, the overall applicability of the introduced ultrasound based navigation system is limited by the presence of the lungs. Additionally, the results confirm the existence of a statistically significant difference between ultrasound transmission through tissue and ribs.

Index Terms—ultrasound, central venous catheter, navigation, real-time.

I. INTRODUCTION

CENTRAL venous catheterization is a well-known technique of accessing the central venous system by cannulating large veins to enable the administration of medications or fluids in cases when standard administration methods are not possible or insufficient [1]. A CVC (*Central Venous Catheter*) can be applied during surgery and/or postoperatively for parenteral nutrition, dialysis, or pain control therapy. To accomplish the successful delivery of medication, the CVC tip needs to be positioned inside the vena cava just above the heart [2].

Current solutions for the CVC navigation and positioning include usage of X-ray or ECG (*electrocardiogram*) technology. In both cases, the CVC is blindly navigated using anatomical indicators. The confirmation of correct position of the CVC can then be verified once at the end of procedure

Dejana Vuković is with the School of Electrical Engineering, University of Belgrade, 73 Bulevar Kralja Aleksandra, 11020 Belgrade, Serbia (e-mail: dejana.vukovic@gmail.com)

Jens Wildhagen is with B. Braun Melsungen AG, Carl-Braun-Straße 1, 34212 Melsungen, Germany (e-mail: jens.wildhagen@bbraun.com)

Korbinian Köhler is with B. Braun Melsungen AG, Carl-Braun-Straße 1, 34212 Melsungen, Germany (e-mail: korbinian.koehler@bbraun.com)

using X-ray or in real-time using ECG [3][4].

In this paper a novel navigation system using ultrasound technology is proposed. The main idea is to transmit ultrasonic signals from the patient's chest and receive them at the tip of the CVC under placement. The time between signal transmission and signal detection shall be used to determine the corresponding distance and calculate the position of the catheter tip in relation to the patient's anatomy [5]. It was expected that for ultrasound frequencies between 10 kHz and 750 kHz the developed system will enable transmission of ultrasound signals through lungs (air) and bones [6][7]. In comparison to X-ray and ECG techniques, the introduced system should ensure a reliable real-time CVC navigation unaffected by changes in physiological signals, which is not dependent on the applicant's skills and is not exposing the patient to unnecessary X-ray radiation.

This paper provides deeper insight into the possibility of ultrasound transmission through the human chest. It introduces an idea for a new and original CVC navigation system and investigates its applicability in the real-life environment.

II. THE METHOD

The implementation of the developed system included realization of a suitable hardware, a model of the upper part of the human torso and appropriate signal processing techniques.

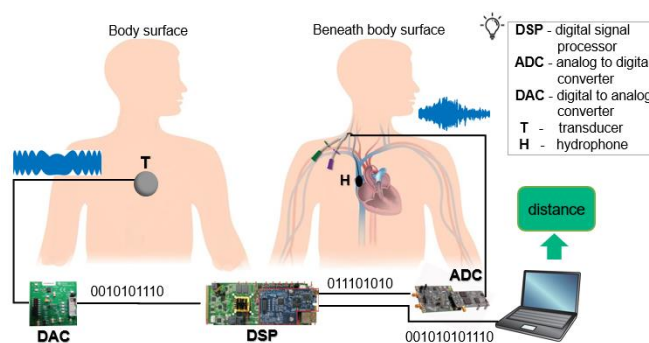


Fig. 1. Schematics of the implemented system.

A. Hardware

The technical part of the system comprising of evaluation boards for DSP (*Digital Signal Processor*) - TMDSEVM6657LS (fixed and floating point, dual core, 1 GHz CPU speed per core), DAC (*Digital to Analog Converter*) - DAC80504EVM (16-bit) and ADC (*Analog to Digital Converter*) - ADS8920BEVM-PDK (16-bit), all manufactured by Texas Instruments (Dallas, Texas, USA),

was responsible for the real-time signal generation and processing. The communication between DSP and data converters was established using a 41.67 MHz SPI (*Serial Peripheral Interface*) channel of the DSP. The sampling rate of the implemented system was 306.7 kHz. An ultrasound transducer of frequency 100 kHz, bandwidth 16 kHz, diameter 40 ± 0.5 mm, manufactured by Multicom Electronic Components (Leeds, England) was used. The hydrophone used in this project was a miniature probe BII-7186 manufactured by Benthowave Instrument Inc. (Collingwood, Canada). The BII-7186 probe is equipped with a built-in digitally programmable preamplifier and a high pass filter with a cut-off frequency of 30 kHz. The amplification factor used in the project was 40 dB. Schematics of the implemented system can be seen on Fig. 1.

B. Model of upper part of human torso

In order to obtain a model with comparable results in terms of ultrasound transmission through the human chest, raw pork ribs and pork lung were used considering the anatomical similarity as well as the speed of sound. Due to the similarity of the speed of sound in tissue, vein, and water (1540 m/s for tissue and vein, 1493 m/s for water), water was used to model tissue. A plastic rectangular water tank (43 cm/40.3 cm x 27 cm x 34 cm/31 cm) with a silicone membrane (26 cm x 19 cm, thickness 3 mm, speed of sound 990 m/s) was designed as a basic setup, whereas different samples of agar-agar moulds (thickness 2 cm, speed of sound 1547 m/s) with samples of rib or lung were used to establish different transmission mediums (Fig. 2. left). The agar-agar moulds were prepared by dissolving agar-agar powder in cold water (5 g agar-agar per 100 ml water), bringing it to boil, cooling it down for 2 h (at a room temperature of approximately 22 °C), pouring the still liquid solution over the samples of lung (8 cm x 7 cm, thickness 2 cm) or rib (8.8 cm x 1 cm x 0.6 cm) within a rectangular glass container (9 cm x 15 cm x 2 cm) and leaving it to cool down in a refrigerator for another 2 h. The silicone membrane was used on the front part of the water tank to simulate the transmission of ultrasound signals through the skin on the human chest (Fig. 2. right). The influence of the ultrasound attenuation during the transmission from the transducer to the silicone membrane was minimized using conductive gel. The final measurement setup can be seen on Fig. 3.

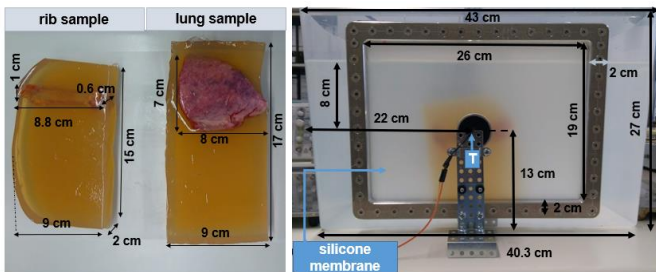


Fig. 2. Left: rib and lung measurement samples with dimensions, right: front view of water tank with silicone membrane, transducer, and rib measurement sample (inside the water tank) including corresponding dimensions.

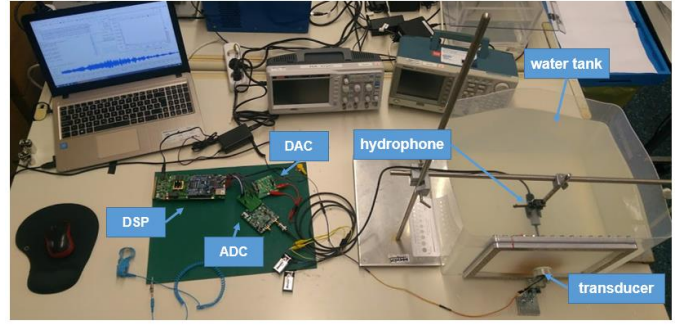


Fig. 3. The final measurement setup.

C. Signal processing

The processing algorithms were developed in C programming language within the CCS v9.1 (*Code Composer Studio*) development environment (Texas Instruments, Dallas, Texas, USA). A block diagram of the implemented signal processing can be seen on Fig. 4.

It has been shown that for frequencies inside the interval from 10 kHz to 750 kHz, the attenuation of the ultrasound signal in lungs decreases as the frequency increases [8], whereas for the transmission of ultrasound through ribs the opposite is valid [7]. The frequency of ultrasound signals used in this project was 100 kHz, chosen as a tradeoff between the conditions mentioned above.

The linear baseband chirp signal with unit amplitude, duration T and frequency sweep (bandwidth) B is defined as follows [9]:

$$m[n] = e^{j2\pi(f_0 nT_s + \frac{K}{2}(nT_s)^2)}, n = \{1 \dots N\} \quad (1)$$

where N is the number of samples of the chirp signal $m(t)$ sampled in the time moments $t = nT_s$, T_s is the sampling period, $K = \frac{B}{T}$, and $f_0 = -\frac{B}{2}$ is the frequency in the time moment $t = 0$. In this project a bandwidth of 16 kHz and a duration of 20 ms have been used.

DSBSC-AM (*Double Sideband Suppressed Carrier - Amplitude Modulation*) of the chirp signal can be formulated as follows [10]:

$$\begin{aligned} s[n] &= \text{Re}\{A_c m[n] e^{j2\pi F_c nT_s}\} \\ &= A_c \cos(2\pi((f_0 + F_c)nT_s + \frac{K}{2}(nT_s)^2)) \end{aligned} \quad (2)$$

where F_c is the frequency of the carrier wave with the amplitude A_c (here: $F_c = 100$ kHz, $A_c = 1.25$ V). Due to characteristics of the used DAC, the transmitted signal was a unipolar value of the modulated signal, as given per:

$$t[n] = s[n] + 1.25 \quad (3)$$

The removal of the DC (*Direct Current*) component of the received signal (present due to characteristics of the used ADC) is performed as follows:

$$r[n] = r_n[n] - r_{DC} \quad (4)$$

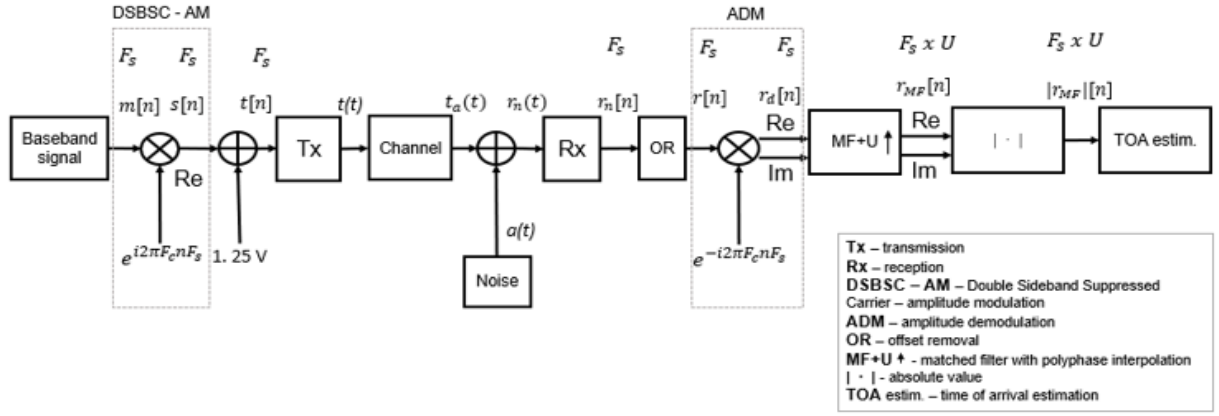


Fig. 4. Block diagram of implemented processing techniques.

$$r_{DC} = \frac{1}{N} \sum_{n=1}^N r_n[n] \quad (5)$$

$$r_n[n] = r_n(nT_s) \quad (6)$$

$$r_n(t) = t_a(t) + a(t) \quad (7)$$

$$t_a(t) = B_c \cos(2\pi((f_0 + F_c)t + \frac{K}{2}t^2)) \quad (8)$$

where $r_n[n]$ are samples of the signal $r_n(t)$, obtained as the sum of the received attenuated signal $t_a(t)$ with amplitude B_c and the noise $a(t)$ in time moments $t = nT_s$, r_{DC} is the estimated DC component, $r[n]$ are samples of the received signal obtained after the removal of the DC component r_{DC} .

The process of amplitude demodulation of the passband chirp signal can be formulated as follows [10]:

$$\begin{aligned} r_d[n] &= r[n] e^{-j2\pi F_c n T_s} \\ &= \frac{B_c}{2} e^{j2\pi(f_0 n T_s + \frac{K(nT_s)^2}{2})} + \frac{B_c}{2} e^{-j2\pi((f_0 + 2F_c)n T_s + \frac{K(nT_s)^2}{2})} \\ &\quad + (a[n] - r_{DC})(\cos(2\pi F_c n T_s) - j \sin(2\pi F_c n T_s)) \end{aligned} \quad (9)$$

where $r_d[n]$ are the samples of the received demodulated signal.

Matched filtering generates its output by correlating a known template signal with the input signal. It is analogue to convolving the input signal with a complex-conjugated and time inverse version of a known template signal [11]. The output of the matched filter is defined as:

$$r_{MF}[n] = r_d[n] * h[n] = \sum_{i=1}^N r_d[i] h[n-i] \quad (10)$$

where $h[n] = m^*[-n]$ is the impulse response of the matched filter corresponding to the complex-conjugated time inverse version of the baseband chirp signal with a duration of N samples.

The output of the matched filter in an ideal noiseless case for a chirp signal as defined per (10) is:

$$\begin{aligned} r_{MF}[n] &= \frac{1}{\pi K n T_s} \sqrt{\frac{jB}{T}} \sin(\pi B n T_s) e^{j2\pi(f_0 n T_s - \frac{K(nT_s)^2}{2})} \\ &= \sqrt{TB} \frac{\sin(\pi B n T_s)}{\pi B n T_s} \sqrt{j} e^{j2\pi(f_0 n T_s - \frac{K(nT_s)^2}{2})} \end{aligned} \quad (11)$$

where $\sqrt{\frac{jB}{T}}$ represents scaling factor resulting from frequency response of a compression filter in a form of a dispersive delay line that enables an ideal compression of chirp signal.

The magnitude of the matched filter output is therefore:

$$|r_{MF}[n]| \approx \sqrt{TB} \frac{\sin(\pi B n T_s)}{\pi B n T_s} \quad (12)$$

and represents a form of a standard *sinc* function.

In order to increase the resolution of the matched filter output, a polyphase interpolation was used. The polyphase interpolation implements a parallel bank of polyphase FIR (*Finite Impulse Response*) filters, whose impulse responses within matched filtering are upsampled values of the template signal. If the factor of interpolation is U , then for each sample of input signal the interpolation filter will provide U new values between successive samples of the interpolated signal [12]. The interpolation factor used in the project was 6.

The time of arrival of a transmitted signal was calculated as follows:

$$\tau_{TOA} = \tau_E - \tau_0 \quad (13)$$

$$\tau_0 = \tau_{EC} - \tau_c \quad (14)$$

$$\tau_c = \frac{d_c}{c_c} \quad (15)$$

where τ_E and τ_{EC} are the time moments corresponding to the measured peak of magnitude of matched filter output during experimental measurement and calibration and τ_c the correct time delay expected for a distance d_c during calibration in a transmission medium with the speed of sound c_c . The peak of the magnitude of the matched filter was estimated using a simple algorithm for signal maximum computation. Additionally, τ_0 denotes the time offset in time of arrival estimation introduced by the system (DAC-ADC conversion, transducer maximum amplitude rise time). The estimation of the distance d was defined as:

$$d = \tau_{TOA} c \quad (16)$$

where c is the speed of sound in the transmission medium [5].

D. Testing of system and statistical analysis

The robustness of the system was estimated by observing the SNR (*Signal-to-Noise Ratio*) in correspondence to the change in the transmission medium and the distance between transmission and reception. The SNR was defined as:

$$SNR_{dB} = 20 \log_{10} \frac{A_1}{A_2} \quad (17)$$

where A_1 and A_2 stand for the magnitude of the strongest and the second strongest peak in the output of the matched filter.

The relative error of distance measurement e_r was estimated using the following relation:

$$e_r = |d_m - D|/D \quad (19)$$

where d_m is the measured distance and D is the exact distance between transducer and hydrophone. The exact distance was measured using a ruler (resolution 1 mm) positioned at the bottom of the water tank by measuring the distance between the marked center of the transducer on the inner part of the silicone membrane and the tip of the hydrophone, which were aligned prior to the measurement.

System testing with different mediums on different distances has been realized using testing conditions shown in Table I. For each of the testing conditions 30 repetitions have been performed.

TABLE I. TESTING CONDITIONS

Medium	F_c [kHz]	B [kHz]	T [ms]	D [cm]
Tissue	100	16	20	5
Rib				10
Lung				20

After obtaining samples for all of the previously described testing conditions, statistic descriptors (mean, standard deviation, median, variance, range, interquartile range, skewness, kurtosis) have been computed using the SSPS v. 27 (*Statistical Package for the Social Sciences*) software package (IBM, Armonk, New York, USA).

The existence of a statistically significant difference between samples of distance estimation in different mediums was examined using the Wilcoxon signed rank test. It tests the hypothesis that the difference of samples of two vectors of data comes from a distribution with a zero median. The result of the test is 1 if it successfully rejects the hypothesis at 5 % significance level, and 0 otherwise. For the implementation in the project the built-in MATLAB (MathWorks, Natick, Massachusetts, USA) function *signrank* was used.

The speed performance of the system was verified by 30 repetitive measurements of the number of clock cycles needed for an execution of the implemented processing algorithm.

III. MAIN RESULTS

Results of the signal processing described in Section II in case of a generated baseband chirp signal with a bandwidth of

16 kHz, a duration of 20 ms, a modulation with carrier on a frequency of 100 kHz and a transmission through the testing medium tissue on a distance of 5 cm, can be seen on Fig. 5-9.

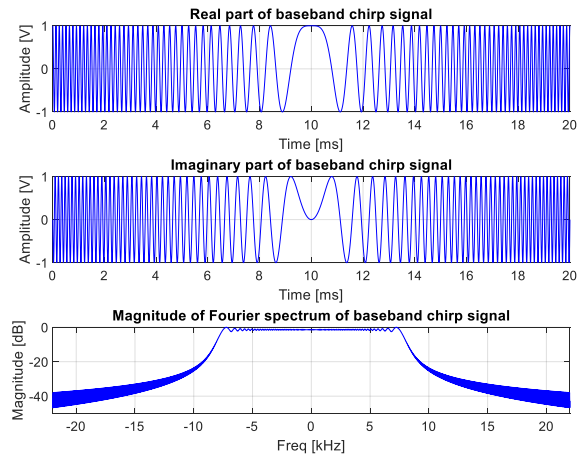


Fig. 5. Baseband chirp signal $m[n]$ with bandwidth 16 kHz and duration 20 ms (top to bottom): real part, imaginary part, magnitude of Fourier spectrum.

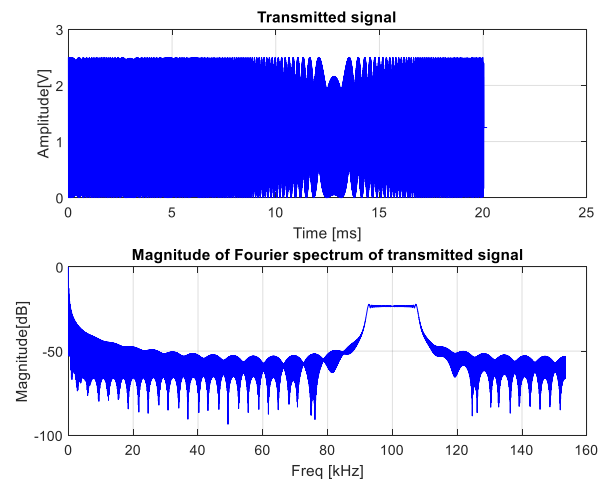


Fig. 6. Transmitted signal $t[n]$ (baseband chirp signal after modulation with carrier on frequency 100 kHz and DC component addition, top to bottom): real part, magnitude of Fourier spectrum.

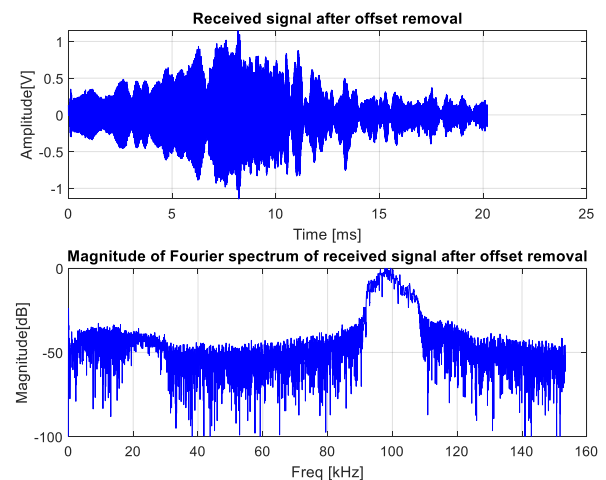


Fig. 7. Received signal $r[n]$ after DC offset removal in case of transmission through testing medium tissue on distance 5 cm (top to bottom): time domain, magnitude of Fourier spectrum.

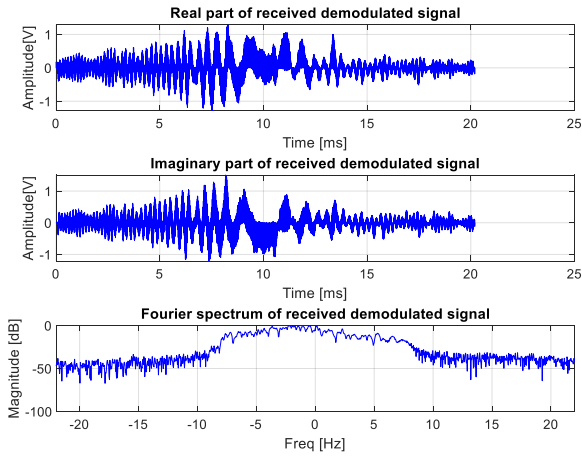


Fig. 8. Received signal without DC component after demodulation with carrier on frequency 100 kHz - $r_d[m]$, in case of transmission through testing medium tissue on distance 5 cm (top to bottom): real part, imaginary part, magnitude of Fourier spectrum.

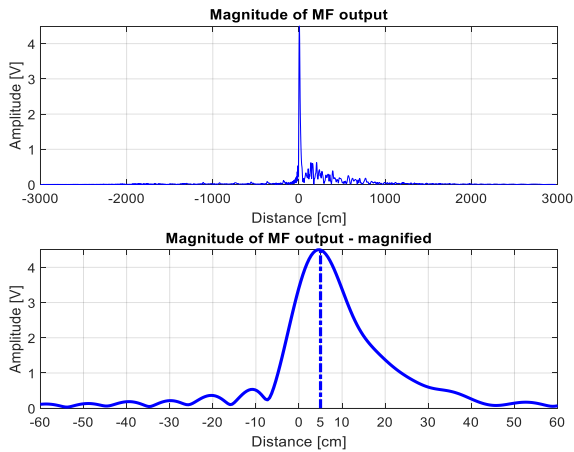


Fig. 9. Magnitude of matched filter output of received demodulated signal without DC offset and baseband chirp signal - $|r_{MF}[m]$ (top to bottom): all samples, magnified section [-60 cm, 60 cm].

Fig. 7. shows that the DC offset component on 0 kHz was successfully removed. Additionally, Fig. 7. (bottom) indicates that there is a substantial amount of noise present on all components of the spectrum.

Fig. 9. (top) shows that the matched filter output in case of a transmission through the testing medium tissue on 5 cm contains several smaller peaks originating from the reflection of the sides of water tank besides the most prominent peak. Fig. 9. (bottom) indicates that the most prominent peak corresponds to the 5 cm distance (the exact distance between the points of transmission and reception).

SNR characteristics (mean values with confidence intervals) obtained during the transmission of chirp signals with a bandwidth of 16 kHz, a duration of 20 ms, modulated with carrier on a frequency of 100 kHz in testing mediums tissue and rib on distances of 5 cm, 10 cm, and 20 cm can be seen on Fig. 10. It shows that as the distance between the points of transmission and reception increases, the estimated SNR decreases. Additionally, the introduction of a rib results in an additional loss of SNR of approximately 4 dB.

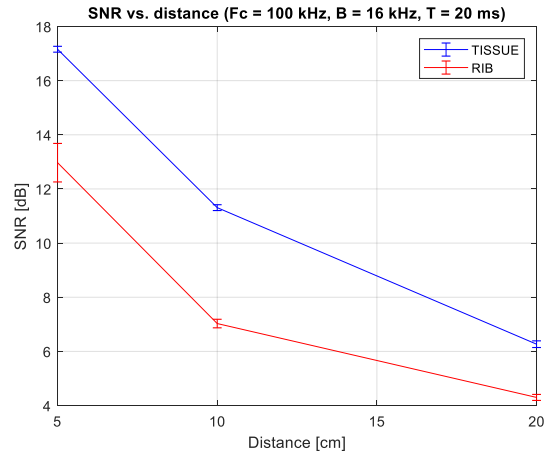


Fig. 10. SNR characteristics in case of transmission of ultrasound signals of frequency 100 kHz, with bandwidth 16 kHz, duration 20 ms in testing medium tissue and medium rib for distances 5 cm, 10 cm, and 20 cm.

The overlapped output of the matched filter and the fraction of the first millisecond of the received signal after offset removal in case of a transmission through testing medium lung on 5 cm can be seen on Fig. 11. The graphs indicate that the most prominent peak does not correspond to the exact distance of 5 cm (approx. 115 cm). As it is not known whether the ultrasound travels through the connective tissue of the lung or through a lot of air-tissue interfaces, it is difficult to estimate whether one of the smaller peaks prior to the most prominent one corresponds to the indirect path through the lungs. Considering that the first peak is present at approximately 17 cm and that the distance from the transducer to the water surface above the water tank is 8 cm (Fig. 2. (right)), this peak could be the result of a surface reflection.

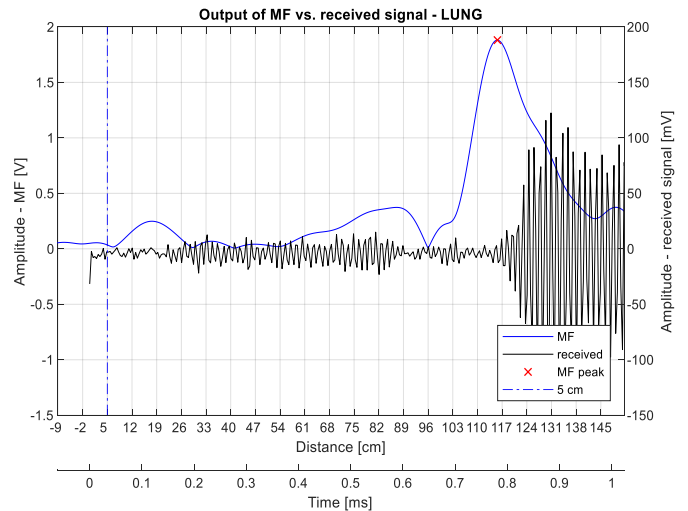


Fig. 11. Overlapped magnitude of matched filter output of received demodulated signal without DC component and baseband chirp signal (blue line) and received signal after DC offset removal (black line) obtained during transmission of ultrasound signals in testing medium lung on distance 5 cm.

The values of the statistic descriptors for the relative error of distance estimation during transmission within the testing medium tissue on distances of 5 cm, 10 cm, and 20 cm can be seen in Table II, whereas comparative values of statistic descriptors for the distance estimation during transmission

within the testing mediums tissue and rib on an exact distance of 5 cm can be seen in Table III.

TABLE II. RELATIVE ERROR OF DISTANCE ESTIMATION DURING TRANSMISSION IN TESTING MEDIUM TISSUE ON DISTANCES 5 CM, 10 CM, AND 20 CM

Descriptor	e_r		
	$D = 5$ cm	$D = 10$ cm	$D = 20$ cm
Mean [%]	0.36	0.62	1.66
Median	$3.67 \cdot 10^{-3}$	$8.86 \cdot 10^{-3}$	$1.67 \cdot 10^{-2}$
Variance	$0.68 \cdot 10^{-3}$	0.14	$0.28 \cdot 10^{-1}$
Std. deviation [%]	$0.26 \cdot 10^{-3}$	0.38	0.17
Range	$2.00 \cdot 10^{-3}$	$8.04 \cdot 10^{-3}$	$1.21 \cdot 10^{-2}$
Interquartile Range	0.00	$8.04 \cdot 10^{-3}$	0.00
Skewness	-2.49	-0.74	-3.39
Kurtosis	5.73	1.55	19.95

TABLE III. COMPARISON OF DISTANCE ESTIMATION DURING TRANSMISSION IN TESTING MEDIUMS TISSUE AND RIB ON DISTANCE 5 CM

Descriptor	d_m	
	Tissue	Rib
Mean	5.02	3.35
Median	5.02	3.24
Variance	$1.69 \cdot 10^{-6}$	$2.25 \cdot 10^{-4}$
Std. deviation	$0.13 \cdot 10^{-2}$	0.15
Range	0.01	0.04
Interquartile Range	0.00	0.32
Skewness	-2.49	0.87
Kurtosis	5.73	1.22

The values in Table II show that with the increase in distance the mean value of the relative error also increases. The standard deviation of the relative error < 1 % indicates that there are no significant changes in the repetitive measurements of the received signal. Table III shows lower mean values of the distance estimation for the testing medium rib than medium tissue. This result is corresponding to the theoretical consideration that the speed of sound in bones is bigger than in tissue/water.

Based on the 30 repetitions of clock measurements, it has been calculated that the update rate of the distance estimation was 3.2 GHz (3.2 s).

The Wilcoxon signed rank test on measurements in the testing mediums tissue and rib for a distance of 5 cm shows value 1. Therefore, there is a statistically significant difference between transmissions in these two mediums.

IV. DISCUSSION AND CONCLUSION

Based on the previously shown results the presented system ensures a low error of distance estimation (< 2 %) for

distances up to 20 cm with a relatively reasonable update rate. However, even though the system is usable in the testing mediums tissue and rib, the results of a transmission through the testing medium lung do not give enough information to confirm the premise that a transthoracic transmission on a frequency of 100 kHz is possible as contrary to the expected results, given in [7]. Therefore, the presented system did not prove to be a viable replacement for existing real-time CVC navigation systems.

Besides the limitation resulting from the ultrasound attenuation in lungs, the performance of the prototype was limited by the characteristics and the interconnection of the hardware. The usage of long wires affected the speed of the SPI and the sampling rate of the system. The low amplitude of the transmitted signals has resulted in low sound pressure levels, whereas the narrow bandwidth of the transducer has affected the amplitude of the matched filter output. By increasing the sound pressure levels of the transmitted signals and the usage of wideband transducers within a uniform electronic system, a further investigation of the possibility of transthoracic transmission can be obtained in future attempts.

ACKNOWLEDGMENT

The authors owe gratitude to CoE Pain Control and CVC within the Hospital Care division of B. Braun Melsungen AG (Melsungen, Germany) for providing equipment for research and prototype development. Special acknowledgment is dedicated to Assistant Prof. Milica Janković, PhD, for help and suggestions during the work on this project.

REFERENCES

- [1] R. Taylor, A. Palagiri, "Central venous catheterization", *Crit. Care Med.*, 35(5), pp. 1390-1396, May 2007.
- [2] A. K. Krishnan, P. Menon, S. V. Kumar, "Electrocardiogram-guided Technique: An Alternative Method for Confirming Central Venous Catheter Tip Placement", *JETS*, 11(4), pp. 276-281, Oct. 2018.
- [3] H. Kamalipour, S. Ahmadi, P. Kamalipour, "Ultrasound for Localization of Central Venous Catheter: A Good Alternative to Chest X-Ray", *Anesth Pain Med.*, 6(5), pp. e.38834, Oct. 2016.
- [4] Y. Jeon, H. G. Ryu, J.H. Kim, J.H. Bahk, "Transesophageal echocardiographic evaluation of ECG-guided central venous catheter placement", *Can J Anaesth.*, 53, pp. 978-983, Oct. 2006.
- [5] S. Holm, "Ultrasound positioning based on time-of-flight and signal strength", *2012 International Conference on Indoor Positioning and Indoor Navigation*, Sydney, Australia, 13-15. Nov. 2012.
- [6] W. Lin, Y.X. Quin, C. Rubin, "Ultrasonic Wave Propagation in Trabecular Bone Predicted by the Stratified Model", *Ann Biomed Eng.*, 29, pp. 781-790, Sept. 2001.
- [7] D. Rueter, H. P. Hauber, D. Droeman, P. Zabel, S. Uhling, "Low-frequency Ultrasound Permeates the Human Thorax and Lung: a Novel Approach to Non-Invasive Monitoring", *Ultraschall in der Medizin*, 31(1), pp. 53-62, Feb 2010.
- [8] P. C. Pedersen, H. S. Ozcan, "Ultrasound properties of lung tissue and their measurements", *Ultrasound Med Biol.*, 12(6), pp. 483-499, June 1986.
- [9] Wikipedia, *Chirp*, [Online]. Available: <https://en.wikipedia.org/wiki/Chirp> (10.08.2020.)
- [10] S. A. Tretter, *Communication System Design Using DSP Algorithms*, 3rd ed, New York, USA: Springer, 2008.
- [11] T. T. Mar, S. S. Y. Mon, "Pulse compression method for radar signal processing", *IJSEA*, 3(2), pp. 31-35, 2014.
- [12] M. Popovic, *Digitalni procesori signala [Digital signal processors]*, 3rd ed. Belgrade, Serbia: Academic mind, 2003.